This document is a postprint of the following published document:
https://doi.org/10.1155/2018/1528792
Advances in Materials Science and Engineering. Volume 2018, Article ID 1528792

Experimental analysis of pretensioned CLT-glulam T-section beams

J. Estévez-Cimadevila[1], F. Suárez-Riestra[1], D. Otero-Chans[1], E. Martín-Gutiérrez[1]

(1) University of A Coruña, Department of Architectural, Civil and Aeronautical Building Structures, Campus A Zapateira, 15071, A Coruña, Spain.

Corresponding author: javier@udc.es (Javier Estévez-Cimadevila)

ORCID:https://orcid.org/0000-0002-8460-2097 (Javier Estévez-Cimadevila)
https://orcid.org/0000-0002-8839-5611 (Félix Suárez-Riestra)
https://orcid.org/0000-0003-1738-252X (Dolores Otero-Chans)
https://orcid.org/0000-0001-7464-4288 (Emilio Martín-Gutiérrez)

ABSTRACT: The bending behavior of T-section beams composed of a glulam web and an upper cross-laminated timber flange was studied. The influence of two fundamental factors on the bending strength and stiffness was considered: the wood species used for the webs and pretensioning with unbonded tendons. Sixteen specimens with a 9 m span were tested until failure: eight of them were non- tensioned (4 *Picea abies* webs and 4 *Quercus robur* webs) and the other eight were pretensioned using threaded bars with 20 mm diameter anchored in plates fixed at the ends of the specimens (4 *Picea abies* webs and 4 *Quercus robur* webs). Pretensioning with unbonded tendons showed a clear improvement in the load capacity of the specimens with *Picea abies* webs, while the difference was not significant for the specimens with *Quercus robur* webs. Considering deflection, pretensioning gave the advantage of an initial precamber but also generated slight variations in the stiffness as a result of increasing the portion of the section that was in compression. The variation in the stiffness depended on the relation between the compressive and tensile moduli of elasticity parallel to the grain, and its influence on the deflection was analyzed using a finite element method.

KEYWORDS: Prestressing; Pretensioning; Glulam; CLT; Timber flooring; Wooden structures.

1. Introduction

Pretensioning techniques are widely used for beams and slabs in concrete structures due to their ability to efficiently compensate for the reduced tensile strength of concrete through precompression. The improvement in strength achieved by pretensioning enables the use of thinner sections and provides an efficient solution for controlling material splitting and avoiding excessive deflections. For materials that have a tensile strength similar to or higher than their compressive strength, such as timber or steel, pretensioning offers significantly reduced advantages. Moreover, timber has problems with its long-term behavior; its inherent creep deflection can cause reduce the pretensioning effects over time, decreasing its capabilities. Therefore, the pretensioning technique is rarely used for timber.

Defect-free timber has a higher tensile strength than compressive strength. However, the inherent defects (cracks, knots, grain deviations, etc.) that are present in structural timber reduce its tensile strength. Furthermore, typical bending failure is reached instantaneously after a brittle fracture is caused by tension in the fibers. This phenomenon has motivated research on different reinforcement solutions to improve the bending behavior of timber.

The reinforcement systems that have been used can be divided in two basic typologies: passive and active reinforcement. Passive reinforcement is made of metallic elements [1-3] or fiber reinforced polymers (FRPs) [3-13] that are glued to the timber with structural adhesives. Active reinforcement can be made with unbonded tendons or with bonded tendons that are glued to the timber with adhesives. Active reinforcement has been used to both reinforce frame connections [14-15] and improve the behavior of beams [16-25].

Some authors [20, 24] have studied the loss of prestressing force for LVL and glulam beams prestressed using unbonded tendons. They found a reduction in prestress from 1.4% to 10% for beams loaded parallel to the grain exposed to controlled and uncontrolled environmental conditions. They concluded that controlling the relative humidity would reduce the losses. The use of bonded reinforcements could contribute to reduce the creep deformations in wood members [5].

This paper focuses on using active reinforcement with unbonded tendons. Therefore, an important reference is the experimental study conducted by McConnell et al. [26] regarding straight beams of laminated timber with a rectangular cross section. Their study analyzed the behavior of three types of reinforcement: beams with passive reinforcement of a 12 mm diameter steel bar, post-tensioned beams with an unbonded 12 mm diameter steel tendon and post-tensioned beams with a bonded 12 mm diameter steel tendon. They concluded that post-tensioning with unbonded tendons increased the bending strength by 17.6% and the stiffness by 8.1%. The small effect of pretensioning on the bending stiffness coincides with the results previously obtained by Bohannan [16].

This paper analyzes the bending behavior of T-section beams formed of glulam webs and upper cross-laminated timber (CLT) flanges. This analysis aims to determine the influence of using different wood species with different mechanical properties for the webs and the effect of pretensioning with unbonded tendons on the strength and bending stiffness of beams. The inherent loss of effectiveness of prestressing in a long-term process is assumed, but it is not considered as a determinant for the purpose of this analysis, as it is carried out in conditions of instantaneous loading.

2. Material and methods

2.1. Materials

The characteristics of the materials used in the experimental study were as follows:

1) Glulam webs made of *Picea abies*, with a strength class of GL28 h [27].
2) Glulam webs made of *Quercus robur* sheets LS13 [28]. The physical and mechanical properties provided by the manufacturer are in Table 1.
3) The CLT flanges, CLT90S L3S [29], were 90 mm thick and were composed of three sheets of 30 mm *Picea abies* C24 [30]. The physical and mechanical properties provided by the manufacturer are in Table 2.
4) The connection between the webs and the flanges of the T-sections was made with 410x80x4 mm perforated plates in S235 hot-dip galvanized finish steel. The circular drills of the plates had a diameter of 10 mm spaced at 5 mm. The plates were glued to the wooden specimens with a 2-component polyurethane adhesive.
5) The pretensioning of the specimens was conducted using threaded bars of Y1100H [31] steel with a 20 mm diameter, an elastic limit of f_{pk}=900 N/mm² and a tensile strength of $f_{pmax,k}$=1100 N/mm².

Table 1

Bending strength	$f_{m,k}$	33 MPa
Tensile strength parallel to the grain	$f_{t,0,k}$	23 MPa
Tensile strength perpendicular to the grain	$f_{t,90,k}$	0.6 MPa
Compressive strength parallel to the grain	$f_{c,0,k}$	45 MPa
Compressive strength perpendicular to the grain	$f_{c,90,k}$	8 MPa
Shear strength	$f_{v,k}$	4 MPa
Modulus of elasticity parallel to the grain	$E_{0,mean}$	14400 MPa
Modulus of elasticity parallel to the grain	$E_{0,05}$	12000 MPa
Modulus of elasticity perpendicular to the grain	$E_{90,mean}$	800 MPa
Modulus of elasticity perpendicular to the grain	$E_{90,05}$	660 MPa
Shear modulus	G_{mean}	850 MPa
Shear modulus	$G_{0,05}$	700 MPa
Characteristic density	ρ_k	690 kg/m³

Table 2

Bending strength	$f_{m,k}$	24 MPa
Tensile strength parallel to the grain	$f_{t,0,k}$	14 MPa
Compressive strength parallel to the grain	$f_{c,0,k}$	22 MPa
Shear strength parallel to the grain of the boards	$f_{v,k}$	2.5 MPa
Modulus of elasticity parallel to the grain of the boards	$E_{0,mean}$	12500 MPa
Shear modulus parallel to the grain of the boards	G_{mean}	460 MPa
Characteristic density	ρ_k	420 kg/m³

2.2. Test specimens

2.2.1 Preliminary tests

Two series of nondestructive tests were conducted. The aim of the first test series was to determine the global bending modulus of elasticity ($E_{m,g}$) of the timber used. The following specimens were tested:

1) 4 Picea abies glulam webs with a cross section of 160x210 mm.
2) 4 Quercus robur glulam webs with a cross section of 160x210 mm.
3) 4 CLT planks with a cross section of 600x90 mm.

Four-point bending tests were conducted with a span of 9 m between the supports. The tested specimens were used later to form the T-sections without pretensioning, as described in section 2.2.2.

The purpose of the second preliminary test series was to determine the compressive elastic modulus of the webs parallel to the grain ($E_{c,0}$). The following specimens, which were obtained from the samples previously tested for bending, were tested under centered compression:

1) 4 *Picea abies* glulam specimens of 55x55x330 mm.
2) 4 *Quercus robur* glulam specimens of 55x55x330 mm.

2.2.2 Tests of the T-section specimens

The following characteristics of the T-sections were tested.

(1) *T-sections without pretensioning*. Eight specimens were formed using a glulam web (4 *Picea abies* specimens and 4 *Quercus robur specimens*) and upper CLT flanges (Fig. 1-a). The total length of the specimen was 9160 mm, and the distance between the supports was L=9 m. The geometric characteristics of the T-section were as follows (Fig. 1-b): b_1=600 mm, b_2=160 mm, h_1=90 mm, h_2=210 mm, and H=300 mm.

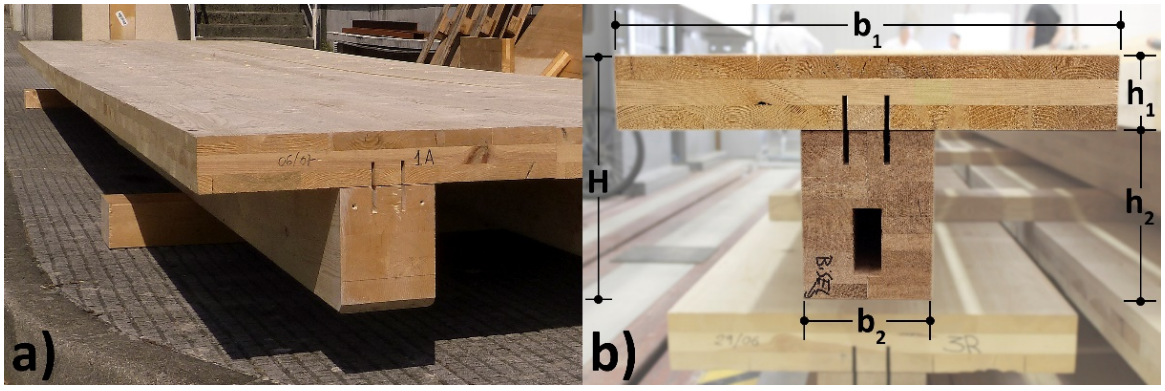

Fig. 1. Picture of a solid transversal section without pretensioning (a) and a piece with a groove prepared to place the pretensioning tendon (b).

The total depth (H) was established by considering the slenderness of the specimen (L/30). A thickness of h_1=90 mm was adopted for the CLT since this is the minimum commercial configuration for 3 plates. The width of the webs (b_2) was determined by considering the restriction of the longitudinal channel in which the tendon was

placed. Finally, the width of the CLT (b_1) was selected to efficiently use the most common commercial dimensions of CLT. The adopted configuration of the T-section enables extending the results to π-shaped sections, a highly efficient typology for constructing structural floors.

The perforated plates of the connection between the web and the flanges (Fig. 2) were placed as shown in Fig. 3-a for the *Picea abies* webs and as shown in Fig. 3-b for the *Quercus robur* webs.

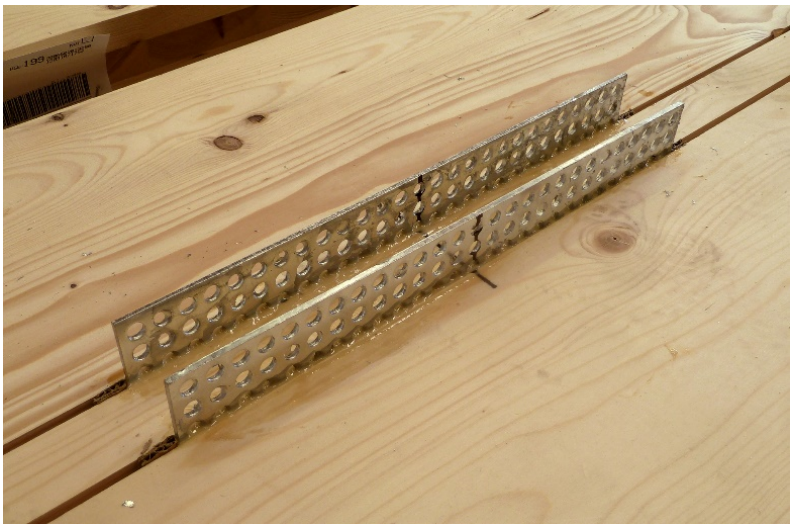

Fig. 2. Discontinuous flange-to-web joint made with glued-perforated steel plates.

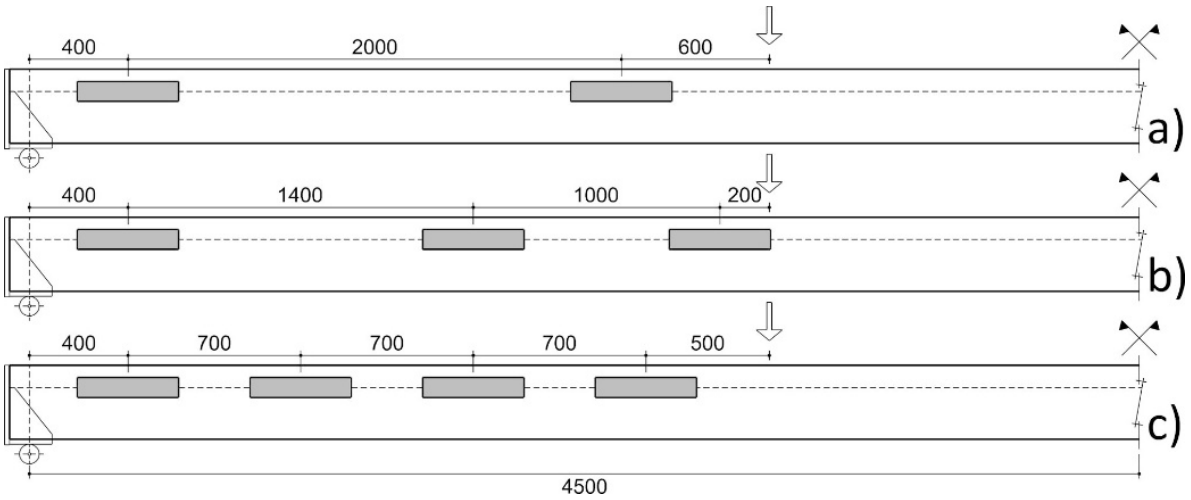

Fig. 3. Dispositions of perforated steel plates adopted according to the type of piece. Non-pretensioned pieces: a) *Picea abies* glulam webs, b) *Quercus robur* glulam webs. Pretensioned pieces: b) *Picea abies* glulam webs, c) *Quercus robur* glulam webs.

To determine the number and distribution of the connection plates, the load capacity of the T-sections with different configurations (the pretensioned and non-tensioned specimens and *Picea abies* and *Quercus robur* webs) was estimated. The load capacity was calculated considering a homogenized section obtained from the material characteristics described in section 2 and assuming a bending failure mode.

A finite element method (FEM) analysis was performed with the obtained load values to assess the required lengths and positions of the connection plates. The adopted distribution proved to be efficient because none of the tested specimens failed at the connection between the web and flange.

(2) *Pretensioned T-sections*. Eight beams were formed with a glulam web (4 *Picea abies* webs and 4 *Quercus robur* webs) and upper CLT flanges with the same characteristics as described for the non-pretensioned beams. The web cross section had a bottom groove or cable channel of 35x85 mm, which was located 30 mm away from the bottom edge, where the tensioning tendon was placed (Fig. 1-b). The vertical dimension of the groove was oversized to accommodate two tendons, which was utilized in another test series using the same specimens. To make the groove, each web was manufactured with two 80 mm wide specimens, and the groove was machined before being glued to form the final 160 mm wide web. The distribution of the perforated plates that connected the web and upper flange is shown in Fig. 3-b (*Picea abies*) and 3-c (*Quercus robur*).

Table 3 shows the geometric characteristics of all the tested specimens.

Table 3. Geometric characteristics of the tested specimens

Type	Wood	Specimen number	Specimen geometry						Test	Tensioning tendon
			L (mm)	H (mm)	h_1 (mm)	h_2 (mm)	B (mm)	b (mm)		Φ (mm)
B/PIC-1 to 4	*Picea abies*	4	9000	---	---	210	---	160	Bending	---
B/OAK-1 to 4	*Quercus robur*	4	9000	---	---	210	---	160	Bending	---
B/CLT-1 to 4	CLT	4	9000	---	90	---	600	---	Bending	---
C/PIC-1 to 4	*Picea abies*	4	330	55	---	---	55	---	Compression	---
C/OAK-1 to 4	*Quercus robur*	4	330	55	---	---	55	---	Compression	---
F1/PIC-1 to 4	T-section with *Picea abies* web	4	9000	300	90	210	600	160	Bending	---
F1/OAK-1 to 4	T-section with *Quercus robur* web	4	9000	300	90	210	600	160	Bending	---
F2/PIC-1 to 4	T-section with *Picea abies* web	4	9000	300	90	210	600	160	Bending	20
F2/OAK-1 to 4	T-section with *Quercus robur* web	4	9000	300	90	210	600	160	Bending	20

2.2.3 Test setup

The preliminary tests conducted to determine the global bending elastic modulus (Fig. 4) and the compression elastic modulus (Fig. 5) considered the general criteria of regulation [32] using a frame with a 600 kN load cell. The bending tests were conducted using a 9 m span between the supports, and point loads were applied at one-third and two-thirds of the span; the midpoint displacement was measured using an extensometer with 100 mm of standard measurement stroke (Fig. 4). The bending elastic modulus parallel to the grain ($E_{0,mean}$) was calculated using equation 1, as shown below.

$$E_{0,mean} = \frac{3 \cdot a \cdot L^2 - 4 \cdot a^3}{2 \cdot b \cdot h^3 \cdot \left(2 \cdot \frac{w_2 - w_1}{F_2 - F_1} - \frac{6 \cdot a}{5 \cdot G_{mean} \cdot b \cdot h} \right)} \quad (1)$$

where a is the distance between a loading point and the nearest support; L is the span of the structural element; b and h are dimensions of the cross section of the beam; F_2-F_1 is the load increase in the straight part of the load-deflection curve and ω_2-ω_1 is the deflection increase corresponding to load F_2-F_1.

Fig. 4. Bending test to determine the global bending MOE.

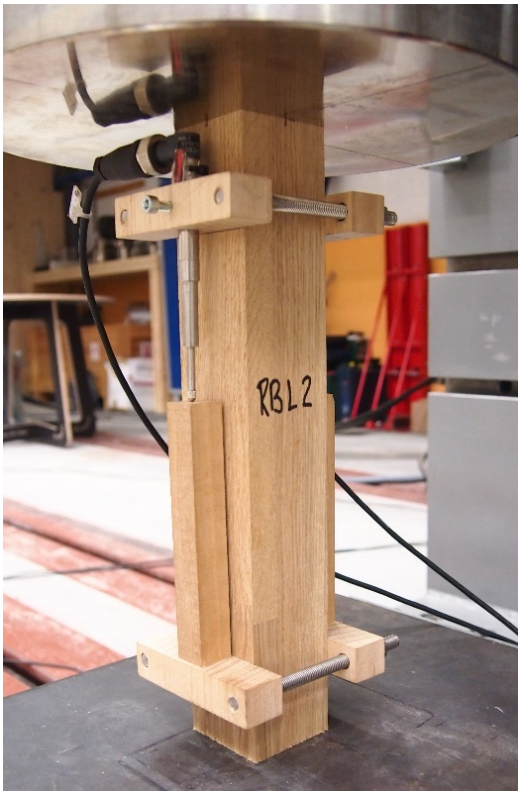

Fig. 5. Test to determine the compression MOE parallel to the grain.

The compression elastic modulus parallel to the grain ($E_{c,0}$) was calculated using equation 2.

$$E_{c,0} = \frac{L_1 \cdot (F_2 - F_1)}{A \cdot (w_2 - w_1)} \quad (2)$$

where L1 is the length, 4 times the smallest dimension of the specimen; F2-F1 is the load increase in the straight part of the load-deflection curve; A is the cross-sectional area of timber and ω2-ω1 is the deflection increase corresponding to load F2-F1.

The T-section was tensioned using a hydraulic jack until a precamber of 18 mm (L/500) was obtained. The tension force applied to reach the precamber was different for each specimen due to their different stiffness. The tendon was locked against the plates using a domed anchor nut [33]. The tendon was placed in the groove of the web 105 mm from the tendon axis to the bottom edge of the specimen (Fig. 6).

Fig. 6. Test of a pretensioned T-section with *Picea abies* webs.

3. Results

Table 4 shows the results that were obtained from the previous tests to determine the modulus of elasticity parallel to the grain for bending and compression. The average value of the global bending modulus of the CLT specimens from the experiments was 6% lower than the one declared by the manufacturer. Compared to the theoretical values listed in section 2, the specimens with *Picea abies* and *Quercus robur* webs exhibited much more significant decreases in the modulus of elasticity (13.7% for *Picea abies* and 17.3% for *Quercus robur*).

Table 4. Modulus of elasticity parallel to the grain

Type	Experimental test series: Value for each specimen (MPa)				Standard deviation	Average value $E_{c,0,\,test}$ (MPa)	Theoretical value: Average value $E_{0,mean,\,test}$ (MPa)	Average value $E_{0,mean}$ (MPa)	$\frac{E_{0,mean,test}}{E_{0,mean}}$
	1	2	3	4					
B/PIC	10880	11450	10510	10658	413	---	10875	12600	0.86
B/OAK	11641	11884	12222	11894	238	---	11910	14400	0.83
B/CLT	10913	11091	12833	12157	908	---	11748	12500	0.94
C/PIC	10208	11365	11115	8616	1244	10326	---	---	---
C/OAK	11676	10767	13375	13248	1264	12267	---	---	---

Table 5 shows the tensioning force applied to each specimen to reach the initial precamber, the maximum force at failure in the bar and the failure load.

Table 5. Force in the tensioning bar and ultimate load

Type	Initial prestressing force, Maximum force in the bar (kN): Specimen				Standard deviation	Average value	Total failure load (sum of the two specific loads applied) (kN): Specimen				Standard deviation	Average value
	1	2	3	4			1	2	3	4		
F1/PIC	---	---	---	---	---	---	55.25	64.15	49.48	61.97	6.67	57.71
F2/PIC	109.20 154.17	117.03 163.79	113.16 176.55	117.89 172.57	3.99 9.95	114.32 166.77	58.15	59.49	95.66	74.18	17.44	71.87
F1/OAK	---	---	---	---	---	---	69.89	87.54	80.36	88.28	8.54	81.52
F2/OAK	115.54 171.81	94.06 147.61	113.29 225.99	116.00 175.49	10.51 32.92	109.72 180.23	73.78	68.92	90.74	84.15	9.88	79.40

Table 6 presents the midpoint displacement of each T-section beam for two point loads of 14 kN; each load was applied at one-third of the span length. In terms of deflection, these point loads were equivalent to a uniformly distributed load of 7 kN/m², which is a common value for public buildings (G_k=2 kN/m² and Q_k=5 kN/m²). The displacements listed in Table 4 do not include the deflection caused by the self-weight of the specimen because the extensometers were installed after the specimen was supported and the load had been applied. In the case of the pretensioned specimens (F2/PIC and F2/OAK), the displacement was measured after pretensioning, so such displacements were measured after some deflection had occurred; therefore, the self-weight was already considered. Thus, to determine the midpoint displacement, the 18 mm of initial precamber was subtracted from the corresponding value in Table 4.

Figs. 7 and 8 show the load-displacement results that correspond to the bending tests of pretensioned and non-tensioned T-sections with *Picea abies* (Fig. 7) and *Quercus robur* webs (Fig. 8). The minimum and maximum values obtained from the action of the two 14 kN loads applied to thirds of the span length are provided. For an

approximately displacement of 15 mm, the load-deflection curves corresponding to the pre-tensioned beams show a clear change in slope caused by the increase of the effective stiffness when the wood comes into contact with the steel bar. This contact occurs when the deformation generated by the beam's self-weight and the loads applied during the test offsets the 18 mm precamber produced by the initial pretensioning force.

Table 4. Displacement at the midpoint of the span for two specific loads of 14 kN applied at 1/3 and 2/3 of the span

Type	Value for each specimen (mm)				Standard deviation	Average value (mm)
	1	2	3	4		
F1/PIC	59.14	56.94	60.14	56.50	1.74	58.18
F2/PIC	64.86	68.63	62.01	64.14	2.76	64.91
F1/OAK	53.29	54.70	57.27	52.89	1.98	54.54
F2/OAK	65.09	63.65	62.09	61.78	1.53	63.15

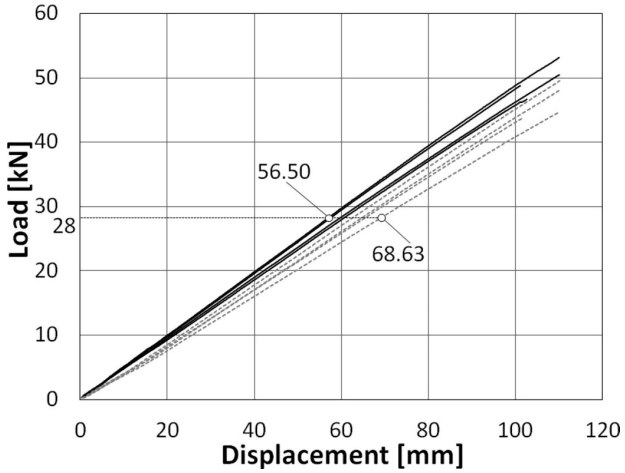

Fig. 7. Load-displacement curves of T-sections with *Picea abies* webs. Pretensioned (dashed lines); non-pretensioned (solid lines).

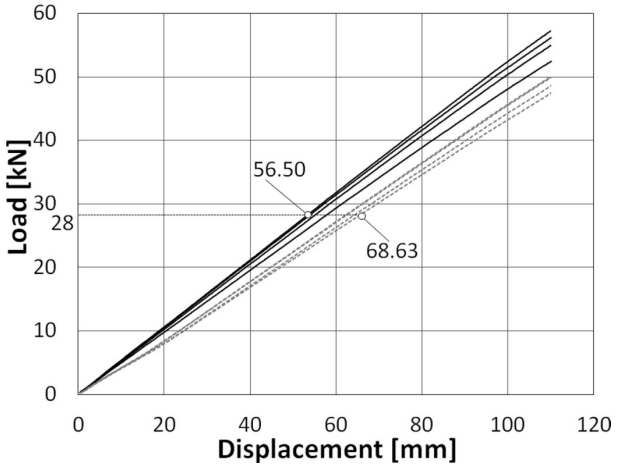

Fig. 8. Load-displacement curves of T-sections with *Quercus robur* webs. Pretensioned (dashed lines); non-pretensioned (solid lines).

The failure of all T-sections, both non-tensioned and pretensioned, occurred instantaneously as a result of the tension in the glulam web. In the non-tensioned specimens, the predominant failure mode was typical glulam bending failure (Fig. 9). In the F1/PIC-3 specimen, the failure was accelerated due to the presence of significant knots in the bottom sheet of the glulam web (Fig. 10). As a result, the failure load of this specimen was the lowest of all the tested specimens (Table 5). Finger-joint failure occurred in the F1/OAK-3 specimen (Fig. 11), and significant variation was not observed in the failure loads of the other tested specimens. In all the pretensioned specimens, with both *Picea abies* and *Quercus robur* webs, typical glulam bending failure was observed (Fig. 12).

Fig. 9. Typical bending failure in non-pretensioned T-sections corresponding to specimen F1/PIC-1.

Fig. 10. Failure due to knots in the specimen F1/PIC-3.

Fig. 11. Failure close to a finger joint in the specimen F1/OAK-3.

Fig. 12. Bending failure in a pretensioned T-section corresponding to specimen F2/OAK-3.

4. Discussion

4.1. Influence of the type of wood used to laminate the web without pretensioning

Using *Quercus robur* laminated timber webs instead of *Picea abies* webs in a non-tensioned beam clearly improves the strength. The average failure load was 81.52 kN for *Quercus robur* and 57.71 kN for *Picea abies*, showing an increase of 41.2%. Moreover, the lowest failure load obtained with the *Quercus robur* webs (F1/OAK-1, 69.89 kN) was 8% higher than the highest value obtained for the *Picea abies* webs (F1/PIC-2, 64.15 kN). Since failure of both the *Picea abies* and *Quercus robur* webs occurred because of tension in the glulam web, the larger strength of the T-section with the *Quercus robur* webs was clearly directly related to the enhanced mechanical properties of the hardwood species. This conclusion can be clearly verified by examining the maximum theoretical stress on the bottom fiber (σ_{bottom}) in Table 5, which was analytically obtained using equation 3 and assuming a pretensioning force (N_{prest}) of zero:

$$\sigma_{bottom} = -\frac{N_{prest}}{A} + \frac{\left(M - N_{prest} \cdot e_{prest}\right) \cdot y}{I} \tag{3}$$

where A is the cross-sectional area of timber; M is the applied moment; e_{prest} is the eccentricity of the pretensioning tendon with respect to the center of mass of the cross section; y is the distance to the neutral axis and I is the moment of inertia of the homogenized section.

The average global modulus of elasticity obtained from the tests on *Quercus robur* webs (11910 N/mm²) was 9.5% higher than that obtained from tests on *Picea abies* webs (10875 N/mm²). Using the *Quercus robur* webs theoretically decreased the bending stiffness (EI) of the homogenized T-section, including the upper CLT board, by 5.6%. The homogenized section was calculated using the average global modulus of elasticity obtained in the tests. The theoretical increase in the bending stiffness (5.6%) was similar than the reduction in the average midpoint displacement of the tested specimens (58.18 mm for the *Picea abies* webs and 54.54 mm for the *Quercus robur* webs). This low increase in the bending stiffness was easily achieved by slightly increasing the depth of the *Picea abies* webs. In the analytical case, the increase in the stiffness provided by using the *Quercus robur* webs could be achieved by increasing

the depth of the *Picea abies* web from 210 mm to 215.7 mm (a 2.7% increase in the depth).

In conclusion, the use of laminated hardwood in the webs of a T-section provides a clear increase only in strength. However, in building structures, the dimensions of simply supported specimens with a medium or long span (the appropriate spans for the type of section analyzed) are not usually determined by strength limitations but by deformation limitations. As a result, the increase in stiffness gained from using glulam hardwood can hardly compensate for the increased cost.

4.2. Influence of pretensioning on the bending strength

Simply supported specimens were pretensioned with unbonded tendons to improve their strength; by applying an eccentric tensioning force, the positive bending generated from exterior loads was reduced. The magnitude of the tensioning force must be limited to ensure that the resultant precamber does not surpass the standard values of service limit states. This limitation in the negative bending magnitude that is induced by pretensioning, together with the additional compressive stresses inherent to tensioning, eliminates the relevance of the increased strength.

Table 5 shows the failure loads of all tested specimens. The specimens with *Picea abies* webs reached an average failure load of 71.87 kN in the pretensioned specimens and 57.71 kN in the non-tensioned specimens. However, this increase of 24.5% must be considered in the context of three issues. First, the small number of tested specimens prevents the results from being conclusive. Second, the low value of the failure load (49.48 kN) of test specimen F1/PIC-3 occurred due to the presence of knots on the bottom side accelerating the failure (Fig. 10). Finally, the high value of the failure load (95.66 kN) reached by test specimen F2/PIC-3 resulted in a standard deviation for the pretensioned specimens (17.44) that was significantly higher than that of the non-tensioned specimens (6.67). The tensioning force applied to the four tested specimens is shown in Table 3. The negative bending moment produced by tensioning was calculated using the global modulus of elasticity of each specimen and the eccentricity of the tendons in relation to the center of gravity of the homogenized sections: 12.83, 13.42, 15.93 and 15.15 kN.m for specimens F2/PIC-1 to 4, respectively. As shown, the largest negative moments (specimens 3 and 4) corresponded to the specimens that reached a higher failure load. However, expressing the negative moment values as a percentage of the isostatic moment produced by the failure load gives the following results: 33.10%, 33.84%, 24.97%, and 30.64% for specimens F2/PIC-1 to 4, respectively. The lowest percentage of the counterbalance moment was produced using specimen F2/PIC-3, which reached the highest failure load, and very significant differences were observed regarding the other specimens.

As a result, since the pretensioning and moment generated by the eccentric pretensioning load were very similar for the 4 specimens, the excellent strength behavior of such specimens could have been a direct consequence of the inherent variations in the mechanical properties of timber. This variation is also reflected in the theoretical tension at the moment of failure (Table 7).

In the specimens with *Quercus robur* webs, pretensioning did not increase the average failure load; these values were even lower than those of the non-tensioned specimens (79.40 kN and 81.52 kN, respectively). Table 7 compares the results in terms of the average theoretical stress at the moment of failure. The tensioning force applied to the four *Quercus robur* test specimens and the maximum force reached by

the tendon are shown in Table 3. The negative bending moments produced by the eccentric tendon at the moment of failure were 13.88, 11.89, 19.16 and 14.71 kN.m for specimens F2/OAK-1 to 4, respectively. The highest value of the counterbalance moment was once again observed in the specimen that reached the highest ultimate load value. This result was also observed when the moments were expressed as a percentage of the isostatic moment at the ultimate load: 28.21%, 25.89%, 31.68% and 26.23%, respectively. The obtained results reveal that the differences in the ultimate loads of the pretensioned and non-tensioned specimens with *Quercus robur* webs were more closely related to the specific material properties than to the influence of pretensioning.

Table 7. Maximum tensile stress estimated for the failure load

Type	Value for each specimen(MPa)				Standard deviation	Average value (MPa)
	1	2	3	4		
F1/PIC	25.75	29.90	23.06	28.88	3.11	26.90
F2/PIC	21.54	21.32	45.67	35.41	11.80	30.98
F1/OAK	33.06	41.41	38.01	41.76	4.04	38.56
F2/OAK	28.67	33.43	44.01	40.81	6.96	36.73

As a result, although it was not possible to reach definitive conclusions, the test results indicate that the benefits of pretensioning on the bending strength of the specimens were not especially relevant. This observation was attributed to the fact that the maximum precamber that could be initially applied with eccentric tensioning was limited by meeting the deflection standards. An efficient way to avoid this limitation in the pretensioning force is to apply a variable tensioning force that generates a counterbalance effect relative to the applied forces. With this goal in mind, the authors developed the SsS© (Self-stressing System) [34, 35].

4.3. Influence of pretensioning on the bending stiffness

Increasing the bending strength of a specimen is not usually the fundamental objective of pretensioning because the dimensions of simply supported specimens are not typically determined by the ultimate limit states but by the service limit states.

The first positive effect provided by pretensioning is to impart precamber to a specimen. In this way, the deflections caused by permanent actions are offset, helping to meet the service restrictions imposed by appearance considerations. Nevertheless, a precamber can be easily imparted in laminated timber during its manufacturing process. Therefore, pretensioning is not necessary if offsetting the deflections caused by permanent loads is the only goal. The other two in-service deflection conditions that must be satisfied are to ensure the integrity of the construction elements and user comfort. The essential parameter for fulfilling both requirements is the bending stiffness of the element; this aspect is especially relevant for high live loads.

The stiffness of the pretensioned specimens, with both *Picea abies* and *Quercus robur* webs, was clearly inferior to that of the non-tensioned specimens, as shown in Figs. 7 and 8. Table 5 shows the midpoint displacement values for a total load of 28 kN (2 loads of 14 kN applied at one-third and two-thirds of the span length, which are equivalent in deflection to a uniform distributed load of 7 kN/m^2). The average displacement value for the specimens with *Picea abies* webs was 64.91 for the pretensioned specimens and 58.18 mm for the non-tensioned specimens,

representing an 11.6% increase in deflection. In the case of *Quercus robur*, the average displacement was 63.15 mm for the pretensioned specimens and 54.54 for the non-tensioned specimens; thus, pretensioning increased the deflection by 15.8%. Thus, compared to the equivalent non-tensioned specimens, the pretensioned specimens with unbonded tendons presented an effective loss in the stiffness, which was attributed to several factors.

The first factor that could have influenced the obtained deflection results is the use of different plate configurations for the flange-web joint of the two species. The distribution of these connection plates was determined to prevent failure at the joint, which would distort the intended analysis. According to the previous joint design, such failure did not occur; therefore, possible slip or failure was not a determining factor in comparing the results. Finally, the pretensioned specimens experienced a higher deflection than the non-tensioned specimens, despite the pretensioned specimens having more connection plates in the flange-web joint.

The second factor that could explain the obtained deflection results is the lower moment of inertia in the pretensioned section because of the groove for the tendon. The groove, as mentioned previously, was vertically oversized to allow for other tensioning configurations. In the specimens with *Picea abies* webs, the decrease in the bending stiffness (EI) of the homogenized section was 7.6%. The precamber of the non-tensioned specimens measured from the tests was 58.18 mm, so the decrease in the stiffness caused by the groove could theoretically improve that value to a maximum of 62.60 mm. However, the total displacement obtained in the pretensioned specimen was 64.91 mm, representing an additional increase of 3.7%.

In the specimens with *Quercus robur* webs, the decrease in the bending stiffness of the homogenized section, calculated with a modulus of elasticity of 11910 MPa, was 7.4%. However, that loss did not correspond to the clearly higher displacements that were measured in the tests, indicating a greater decrease in stiffness. Preliminary tests to determine the modulus of elasticity were conducted using the same webs that were used to make the non-tensioned T-section specimens. The average modulus of elasticity was 11910 MPa in the *Quercus robur* web and 10875 MPa in the *Picea abies* web. Surprisingly, the pretensioning force needed to obtain a precamber of 18 mm was lower in the specimens with *Quercus robur* webs (109.72 kN) than in the specimens with *Picea abies* webs (114.32 kN). This result can be explained by considering that the timber of the webs in the pretensioned specimen had a lower modulus of elasticity. Given that we know the moment of inertia, tensioning force and precamber for each of the F2/OAK specimens, we obtained an average modulus of elasticity of 10090 MPa. As a result, a 16.49% decrease in stiffness was generated by the groove combined with the reduction in the modulus of elasticity E_m (from 11910 to 10090 MPa). This decrease in the stiffness increased the average precamber value from 54.54 mm, obtained for the solid specimen, to 63.53 mm in the specimen with the groove. This value is slightly higher than that obtained from the tests (63.15 mm, as shown in Table 8).

Finally, the third factor that explains the obtained displacement results was attributed to the differences between the modulus of the compressive modulus of elasticity ($E_{c,0}$) and the tensile modulus of elasticity ($E_{t,0}$) parallel to the grain. The pretensioning of the section increased the compressive stresses and consequently increased the compression area of the section. This is, the normal bending stresses that originated from the eccentric pretensioning and external force, combined with the normal compressive stresses due to pretensioning, led to a displacement in the

neutral fiber that increased the compression area. Depending on the relative values of the tensile modulus of elasticity and the compressive modulus of elasticity, the increase in the compression section led to a slight decrease (if $E_{c,0} < E_{t,0}$) or increase (if $E_{c,0} > E_{t,0}$) in the stiffness.

Table 8. Displacement at the midpoint of the span for two point loads of 14 kN applied at 1/3 and 2/3 of the span

Type	Pre-tensioning force kN	Displacement Experimental test (mm)	Modulus of elasticity (MPa)			Displacement FEM (mm)	
			E_m	$E_{c,0}$	$E_{t,0}$	With global modulus of elasticity E_m	With bimodulus $E_{c,0}$ and $E_{t,0}$
F1/PIC	---	58.18	10875	10326	11470	58.98	58.95
F2/PIC	---	---	10875	10326	11470	63.56	63.51
	114.32	64.91 (18.00+46.91)	10875	10326	11470	63.48 (17.27+46.21)	65.64 (18.26+47.38)
F1/OAK	---	54.54	11910	12267	11570	55.25	54.81
F2/OAK	---	---	10090	10390	9800	66.47	65.25
	109.72	63.15 (18.00+45.15)	10090	10390	9800	64.77 (17.22+47.55)	63.67 (17.38+46.29)

To verify the proposed theory, an FEM analysis for solid specimens (types F1/PIC and F1/OAK) and specimens with grooves (types F2/PIC and F2/OAK) was conducted, considering both non-tensioned and pretensioned specimens.

Three-dimensional models of hexahedral finite elements with 8 nodes containing 24 degrees of freedom (DOFs) were generated. The contact between the elements accounted for the possibility of dynamic behavior from flexible and/or rigid components, with kinematic restrictions on relative movement (displacement and rotation) between the nodes that formed the connection.

Two cases were assumed for the material properties. In the first case, the global modulus of elasticity was considered. In the second case, a bimodulus material was used to define not only the different elastic moduli for both compression and tension but also the different stress-strain curves for compression and tension.

The global bending modulus of elasticity ($E_{0,mean,\ test}$) and compression modulus of elasticity parallel to the grain ($E_{c,0,test}$) were determined in previous tests (Table 2). Using equation 4 [36], which is well known for determining the virtual modulus of elasticity (E_m) in softwood, we estimated the tensile modulus of elasticity parallel to the grain ($E_{t,0}$), using the global modulus obtained from the tests ($E_{0,mean,\ test}$) as the virtual modulus (E_m):

$$E_m = \frac{4 \cdot E_{t,0} \cdot E_{c,0}}{\left(\sqrt{E_{t,0}} + \sqrt{E_{c,0}}\right)^2} \tag{4}$$

Table 8 shows the average displacement values obtained from the experimental tests and those obtained from the numerical analysis. For the pretensioned specimens, the

precamber generated by the pretensioning plus the midpoint displacement is noted in parentheses in this table.

The numerical analysis conducted using the virtual modulus of elasticity (E_m) and the bimodulus ($E_{c,0}$ and $E_{t,0}$) led to interesting conclusions. In the case of the non-tensioned specimens, for both the solid section and the section with a groove in the web, the analysis results using the bimodulus showed a high correlation with the results obtained using the virtual modulus of elasticity. This correlation was very similar for the specimens with *Picea abies* webs and was slightly lower for the specimens with *Quercus robur* webs; hence, we recommend checking equation 4 when using it for hardwood. In contrast, in the case of the pretensioned specimens, the results obtained using the bimodulus were clearly closer to the experimental results than were the results from the analysis using the virtual modulus. The displacement of the pretensioned specimen with *Picea abies* webs obtained from the numerical model (65.64 mm) was 11.3% higher than that of the non-tensioned solid specimen (58.95 mm). In the experimental tests, this increase was 11.6% (64.91 mm for the pretensioned specimen and 58.18 mm for the non-tensioned specimen). In the specimens with *Quercus robur* webs, the displacement in the numerical model increased by 16.2%, which was practically the same as the increase obtained from the tests (15.8%). These results confirm that the variations in the stiffness experienced by the specimens under tension were a consequence of the significant increase in the compression area of the section (Fig. 13). To help visualize the pretensioning phenomenon, the areas with tensile stress, regardless of the magnitude, are shown in red in Fig. 13.

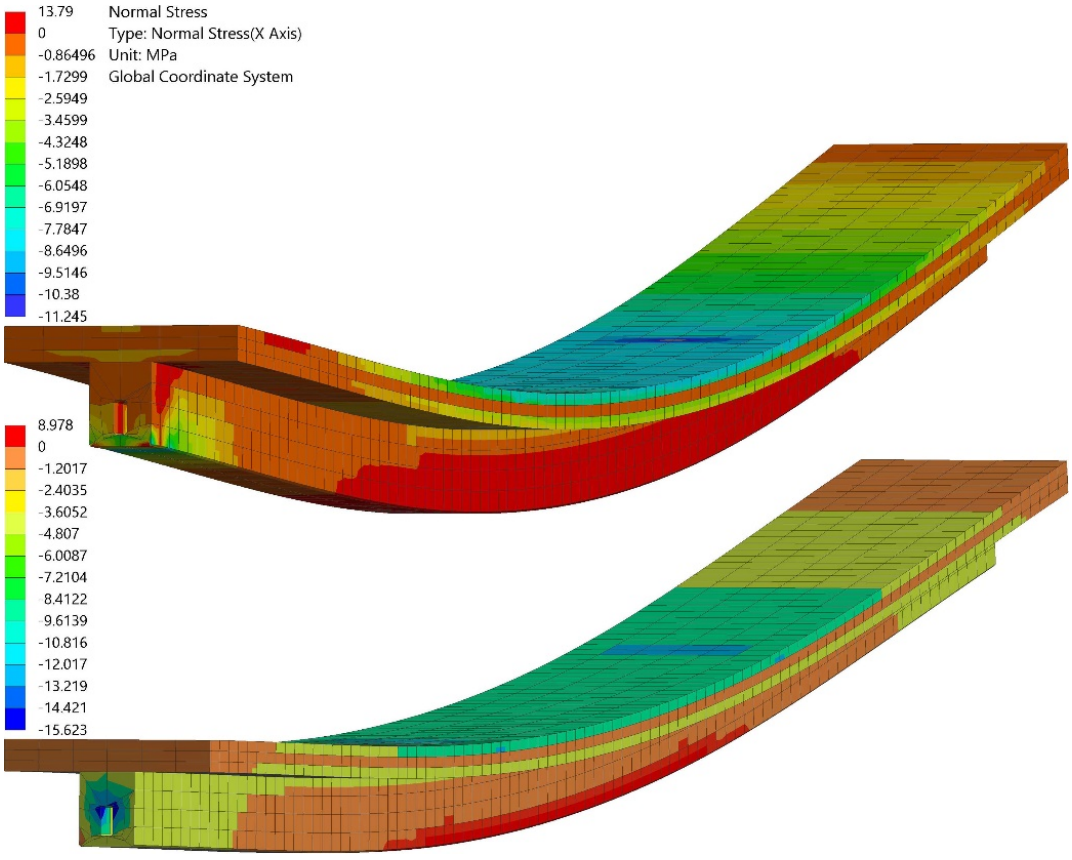

Fig. 13. Finite Element Model. Visualization of the increase of the compressed zone in pieces of T-section with *Picea abies* webs, pretensioned (bottom) and non-pretensioned (top).

The results presented here significantly differ from those obtained by McConell et al. [26]. In our experimental tests, the pretensioned *Picea abies* specimens showed an 11.6% higher deflection than the non-tensioned specimens. This 11.6% increase was reduced to 3.7% after disregarding the loss of inertia due to the groove where the tendon was placed. Conversely, in the tests conducted by McConell et al. [26], the pretensioning reduced the deflection by 8.1%. This disagreement was attributed to the interactions of several factors. First, the tendon was placed much closer to the edge of the specimen (22.5 mm instead of 105 mm). Second, the size of the tested specimens were different (sections of 45x145 mm with a 3 m span facing the T-sections with a 300 mm depth and 9 m span). Third, there were possible differences in the relation between the compressive and tensile moduli of elasticity parallel to the grain of the timber used in the tests. The above mentioned circumstances could generate a greater rotational restraint at the edges of the specimens to reduce the deflection. Moreover, the benefit of pretensioning indicated by McConell's experiments was also small.

5. Conclusions

Using *Quercus robur* instead of the usual *Picea abies* for laminating the webs of T-section specimens led to a 41.2% increase in the bending resistance and a 5.6% increase in stiffness. Given that the dimensions of simply supported specimens with a medium or long span are normally determined by deflection limitations, *Quercus robur* is generally not used due to its high cost and small benefit. The 5.6% increase in stiffness obtained in the tests could be achieved by increasing the depth of the *Picea abies* web by only 2.7%.

Pretensioning the T-sections increased the bending strength by 24.5% for the specimens with *Picea abies* webs. The average failure load of the T-sections with *Quercus robur* webs was lower in pretensioned specimens than in the non-tensioned specimens, even though the difference was only 2.6%.

The bending stiffness is a fundamental property for dimensioning simply supported specimens, and pretensioning slightly varied the stiffness of the section because of the increased compression area. We proved that such stiffness variations depend on the relation between the compressive and tensile moduli of elasticity parallel to the grain. In the analyzed cases, we found a 3.7% decrease in the stiffness of the specimens with *Picea abies* webs and a very slight increase in the specimens with *Quercus robur* webs (discounting the reduction due to the groove).

Due to the number of tested specimens and the use of different configurations for the flange-web joints with glued-perforated steel plates, we advise conducting another experimental test series to confirm the obtained conclusions.

Acknowledgments

This research is part of the research project "High-performance prefabricated systems made of prestressed laminated wood without adhered tendons" financed by the Spanish Ministry of Economy and Finance and the European Regional Development Fund (ERDF).

References

[1] A. Borri and M. Corradi, "Strengthening of timber beams with high strength steel cords," Composites: Part B, vol. 42, no. 6, pp. 1480–1491, 2011. http://doi.org/10.1016/j.compositesb.2011.04.051.

[2] J. Soriano, B. P. Pellis, and N. T. Mascia, "Mechanical performance of glued-laminated timber beams symmetrically reinforced with steel bars," Composite Structures, vol. 150, pp. 200–207, 2016. http://doi.org/10.1016/j.compstruct.2016.05.016.

[3] H. Yang, W. Liu, W. Lu, S. Zhu, and Q. Geng, "Flexural behavior of FRP and steel reinforced glulam beams: experimental and theoretical evaluation," Construction and Building Materials, vol. 106, pp. 550–563, 2016. http://doi.org/10.1016/j.conbuildmat.2015.12.135.

[4] N. Plevris and T. C. Triantafillou, "FRP-Reinforced wood as structural material," Journal of Materials in Civil Engineering, vol. 4, no. 3, pp. 300–317, 1992.

[5] N. Plevris and T. C. Triantafillou, "Creep behavior of FRP-reinforced wood members," Journal of Structural Engineering, vol. 121, no. 2, pp. 174–186, 1995.

[6] T. C. Triantafillou, "Shear reinforcement of wood using FRP materials," Journal of Materials in Civil Engineering, vol. 9, no. 2, pp. 65–69, 1997.

[7] A. Yusof and A. L. Saleh, "Flexural strengthening of timber beams using glass fibre reinforced polymer," Electronic Journal of Structural Engineering, vol. 10, pp. 45–56, 2010.

[8] G. M. Raftery and A. M. Harte, "Low-grade glued laminated timber reinforced with FRP plate," Composites Part B, vol. 42, no. 4, pp. 724–735, 2011.

[9] G. M. Raftery and A. M. Harte, "Nonlinear numerical modelling of FRP reinforced glued laminated," Composites Part B, vol. 52, pp. 40–50, 2013. http://doi.org/10.1016/j.compositesb.2013.03.038.

[10] P. De La Rosa García, A. C. Escamilla, and M. N. González García, "Bending reinforcement of timber beams with composite carbon fiber and basalt fiber materials," Composites Part B, vol. 55, pp. 528–536, 2013. http://doi.org/10.1016/j.compositesb.2013.07.016.

[11] A. D'Ambrisi, F. Focacci, and R. Luciano, "Experimental investigation on flexural behavior of timber beams repaired with CFRP plates," Composite Structures, vol. 108, pp. 720–728, 2013. http://doi.org/10.1016/j.compstruct.2013.10.005.

[12] P. De La Rosa García, A. C. Escamilla, and M. N. González García, "Analysis of the flexural stiffness of timber beams reinforced with carbon and basalt composite materials," Composites Part B, vol. 86, pp. 152–159, 2016. http://doi.org/10.1016/j.compositesb.2015.10.003.

[13] I. Glisovic, B. Stevanovic, and M. Todorovic, "Flexural reinforcement of glulam beams with CGRP plates," Materials and Structures, vol. 49, no. 7, pp. 2841–2855, 2016. http://doi.org/10.1617/s11527-015-0690-7.

[14] T. Smith, F. C. Ponzo, A. Cesare et al., "Post-tensioned glulam beam-column joints with advanced damping systems: testing and numerical analysis," Journal of Earthquake Engineering, vol. 18, no. 1, pp. 147–167, 2014. http://doi.org/10.1080/13632469.2013.835291.

[15] F. Wanninger and A. Frangi, "Experimental and analytical analysis of a post-tensioned timber connection under gravity loads," Engineering Structures, vol. 70, pp. 117–129, 2014. [16] B. Bohannan, "Prestressed wood laminated beams," Forest Products Journal, vol. 12, no. 12, pp. 596–602, 1962.

[16] B. Bohannan, "Prestressed wood laminated beams," Forest Products Journal, vol. 12, no. 12, pp. 596–602, 1962.

[17] T. C. Triantafillou and N. Deskovic, "Prestressed FRP sheets as external reinforcement of wood members," Journal of Structural Engineering, vol. 118, no. 5, pp. 1270–1284, 1992.

[18] C. W. Dolan, T. L. Galloway, and A. Tsunemori, "Prestressed glued laminated timber beam—Pilot study," Journal of Composites for Construction, vol. 1, no. 1, pp. 10–16, 1997.

[19] A. Buchanan, A. Palermo, D. Carradine, and S. Pampanin, "Post-tensioned timber frame buildings," Structural Engineer, vol. 89, no. 17, pp. 24–30, 2011.

[20] M. Davies and M. Fragiacomo, "Long-term behavior of prestressed LVL members. I: experimental tests," Journal of Structural Engineering, vol. 137, no. 12, pp. 1553–1561, 2011. http://doi.org/10.1061/(ASCE)ST.1943-541X.0000405.

[21] V. De Luca and C. Marano, "Prestressed glulam timbers reinforced with steel bars," Construction and Building Materials, vol. 30, pp. 206–217, 2012.

[22] J. Negraˆo, "Prestressing systems for timber beams," in Proceedings of World Conference on Timber Engineering WCTE-12, vol. 1, pp. 252–261, Auckland, New Zealand, July 2012.

[23] W. Van Beerschoten, A. Palermo, D. Carradine, and S. Pampanin, "Design procedure for long-span post-tensioned timber frames under gravity loading," in Proceedings of World Conference on Timber Engineering WCTE-12, vol. 1, pp. 354–361, Auckland, New Zealand, July 2012.

[24] F. Wanninger, A. Frangi, and M. Fragiacomo, "Long-term behavior of posttensioned timber connections," Journal of Structural Engineering, vol. 141, no. 6, article 04014155, 13 pages, 2015.

[25] T. Smith, F. Sarti, G. Granello et al., "Long-term dynamic characteristics of Pres-Lam structures," in Proceedings of World Conference on Timber Engineering WCTE 2016, Vienna, Austria, August 2016.

[26] E. McConnell, D. McPolin, and S. Taylor, "Post-tensioning of glulam timber with steel tendons," Construction and Building Materials, vol. 73, pp. 426–433, 2014. http://doi.org/10.1016/j.conbuildmat.2014.09.079.

[27] EN 14080, Timber Structures. Glued Laminated Timber and Glued Solid Timber, Requirements, European Committee for Standardization (CEN), Brussels, Belgium, 2013.

[28] ETA 13/0642, VIGAM-Glued Laminated Timber of Oak, European Technical Assesment, Brussels, Belgium, 2013.

[29] ETA 14/0349, CLT-Cross Laminated Timber, European Technical Assesment, Brussels, Belgium, 2014.

[30] EN 338, Structural Timber. Strength Classes, European Committee for Standardization (CEN), Brussels, Belgium, 2009.

[31] prEN 10138–4, Prestressing Steels—Part 4: Bars, European Committee for Standardization (CEN), Brussels, Belgium, 2000.

[32] EN 408, 2010+A1, Timber Structures. Structural Timber and Glued Laminated Timber. Determination of Some Physical and Mechanical Properties, European Committee for Standardization (CEN), Brussels, Belgium, 2012.

[33] ETA 05/0123, Dywidag-System International GmbH, European Technical Assesment, Brussels, Belgium, 2013.

[34] J. Estévez-Cimadevila, D. Otero-Chans, E. Martín-Gutiérrez, and F. Suárez-Riestra, "Self-tensioning system for long-span wooden structural floors," Construction and Building Materials, vol. 102, pp. 852–860, 2016. http://doi.org/10.1016/j.conbuildmat.2015.11.024.

[35] D. Otero-Chans, J. Estévez-Cimadevila, E. Martín-Gutiérrez, and J. Pérez-Valcárcel, "Application of a new system of self-tensioning to the design of large-span wood floor framings," Journal of Structural Engineering, vol. 142, no. 6, p. 04016012, 2016. http://doi.org/10.1061/(asce)st.1943-541x.0001486.

[36] V. Baño, R. Argüelles-Bustillo, R. Regueira, and M. Guaita, "Determination of the stress-strain curve in specimens of Scots pine for numerical simulation of defect free beams" Materiales de Construcción, vol. 62, no. 306, pp. 269–284, 2012. http://doi.org/10.3989/mc.2012.64110.

[47] R. Rijal, B. Samali, R. Shrestha, K. Crews, Experimental and analytical study in dynamic performance of timber floor modules (timber beams) 981–399, Constr. Build. Mater. 122 (2016), https://doi.org/10.1016/j.conbuildmat.2016.06.027.